Solid State Ionics 180 (2009) 946–951

Contents lists available at ScienceDirect

Solid State Ionics

journal homepage: www.elsevier.com/locate/ssi

First principle study of structural, phase stabilization and oxygen-ion diffusion properties of β-$La_{2-x}L_xMo_2O_9$ (L = Gd, Sm, Nd and Bi) and β-$La_2Mo_{2-y}M_yO_9$ (M = Cr, W)

Xiang-Shan Kong [a], C.J. Hou [a,b], Qing-Hai Hao [a], C.S. Liu [a,*], X.P. Wang [a], Q.F. Fang [a]

[a] Key Laboratory of Materials Physics, Institute of Solid State Physics, Chinese Academy of Sciences, P.O. Box 1129, Hefei 230031, PR China
[b] School of Science, Jiangxi University of Science and Technology, Ganzhou 341000, PR China

ARTICLE INFO

Article history:
Received 16 January 2009
Received in revised form 20 April 2009
Accepted 24 April 2009

Keywords:
$La_2Mo_2O_9$
Substitution
First principle study
Phase stabilization
Oxygen-ion diffusion
Oxygen-ion conductor

ABSTRACT

We have performed a first principle study of structural and phase stabilization of β-$La_{2-x}L_xMo_2O_9$ (L = Gd, Sm, Nd and Bi) and β-$La_2Mo_{2-y}M_yO_9$ (M = Cr, W). The substitutional-site properties were discussed in terms of the empirical parameter, bond valence sums (BVS), which characterizes the interactions between atoms and its nearest-neighbor atoms and correlates well with the stability of the structure. We found that Gd, Sm and Nd atoms prefer the crystallographic sites with largest BVS values. The nonlinear dependence of cell parameter on W content in W-doped systems results from the nonlinear change in Mo/W–O bond length with W content. The decrease of cohesive energy and the deviation of BVS values from the expected values upon the Gd, Sm, Nd and W-doped concentration help us understand the experimentally observed stabilization of the β phase to lower temperatures in these doped system. The O ion diffusion properties in W-doped systems have been studied using the nudged elastic band method and the dimer method. We found that, W-doping leads to the obvious increase in the energy barriers of O ion concerted diffusion. In addition, there is a remarkable decrease in the difference of energy barriers between two diffusion channels involving O(1) ion, which sheds light on only one relaxation peak in the mechanical relaxation measurement in W-doped system, compared to undoped system.

© 2009 Elsevier B.V. All rights reserved.

1. Introduction

Fast oxide ionic conductors have been attracting much theoretical and practical interest because of their potential application in many different fields such as solid fuel cells, oxygen pumps and membranes for oxygen separation [1,2]. As an oxide-ion conductor originally reported by Lacorre et al. [3], $La_2Mo_2O_9$ has been extensively investigated in the recent years for its excellent anionic conductivity at intermediate temperatures (600–800 °C) and the interesting formation mechanism of oxygen vacancies based on lone-pair substitution concept. However, it undergoes a reversible phase transition from a high-temperature disorder phase β-$La_2Mo_2O_9$ to low-temperature order phase α-$La_2Mo_2O_9$ at 580 °C with an abrupt decrease in ionic conductivity. According to the work by Goutenoire et al. [4], $La_2Mo_2O_9$ has a monoclinic structure (space group P21) at low temperatures and a cubic structure (space group $P2_13$) at high temperatures. Based on the neutron atomic pair distribution function analysis, Malavasi et al. [5] provided evidence that the local structure of β phase is identical with that of α phase, because the structural phase transition $\alpha \rightarrow \beta$ is actually a transition from static to dynamic distribution of the oxygen defects without any shift of heavy atoms. This phase transition greatly limits the potential application of $La_2Mo_2O_9$ as an oxide-ion conductor. In addition, hexavalent molybdenum oxides usually suffer degradation in a highly reducing atmosphere [6], which questions the aging behavior of this compound under the stringent conditions. A number of experimental reports have shown that [7–20] , many dopants substituting for La by L (L = K, Ca, Sr, Ba, Bi, Y, Sm, Nd, Gd, Dy, Er) or Mo by M (M = V, W, Cr) can suppress the $\beta \rightarrow \alpha$ phase transition and thus enable the cubic phase to persist metastably at lower temperature. For example, for the substitution of La by Nd the phase transition temperature decreases about 100 °C when the substitution concentration is above 40%. For the substitutions of La by Gd and Y, above a certain doping level, the suppression of the phase transition and stabilization at room temperature of the cubic β form are achieved. These elements give both chemical and steric possibilities for a large substitution, namely up to 50 and 25% for Nd and Gd [14]. Marrero-López et al. found that the substitution of Mo by W preserving the $La_2Mo_2O_9$ structure is possible up to 75%, whereas the La can be substituted by Nd up to 87.5% [15]. Georges et al. [16] found that Mo substitution by W has a beneficial effect on the stability of the compound in reducing conditions, and the substitution range is wide (up to around 80%) and moreover W suppresses the phase transition by stabilizing the β form at room temperature. In addition, Goutenoire et al. [18] observed an unusual evolution of the cubic cell parameter in

* Corresponding author. Tel.: +86 551 5591062.
E-mail address: csliu@issp.ac.cn (C.S. Liu).

0167-2738/$ – see front matter © 2009 Elsevier B.V. All rights reserved.
doi:10.1016/j.ssi.2009.04.015

the series $La_2Mo_{2-y}W_yO_9$, which was confirmed by Georgers et al. [16]. Corbel et al. [21] presented a study of the influence of Cr and W substitutions on the structural arrangement of $La_2Mo_2O_9$ by employing neutron scattering. They found that, the substitution by Cr appears to have little incidence on the structural arrangement apart from a regular shrinkage of the cell volume due to substitution by a smaller cation; the substitution by W has a more complex nonlinear effect: first, a slight regular increase (W:Mo<1) and then a more abrupt decrease (W:Mo>1) of the cell volume as a function of W content. In our preceding works [22,23], we have theoretically investigated the oxygen-ion arrangements in β-$La_2Mo_2O_9$ and revealed the structure features of β-$La_2Mo_2O_9$. Now we want to extend our study of the structure features and stabilization of high-temperature phase in substituted $La_2Mo_2O_9$.

In addition, the mechanical and dielectric relaxation studies suggested that the oxygen-ion migration path involves all of the three oxygen sites, including the fully occupied O(1) site [24]. However, the large anisotropic thermal parameters and partial site occupancies which characterize the O(2) and O(3) sites of this structure, associated with the short oxygen–oxygen distances between these two atoms, makes the conduction path between O(2) and O(3) more likely [14,25,18,26]. By the *ab initio* MD simulation [22], we supported two diffusion channels: one involves the migration of O(2) ion with low activation energy and short migration length assisted by O(3), and another is the migration of O(3) with large activation energy and long migration length assisted by O(1) and O(2) ions. But the low activation energy (0.5 eV) of the migration of O(2) assisted by O(3) suggests the collective diffusion of O(2) and O(3) ions should not be responsible for the experimentally observed mechanical and dielectric relaxation peaks. So only one of these two diffusion channels is related to two relaxation peaks observed in the mechanical relaxation measurement, which questions the correlation between the collective diffusion of O(1) and O(2) and O(3) ions and two relaxation peaks. Recently, the W-substituted $La_2Mo_2O_9$ have been systematically investigated using the internal friction technique and the dielectric relaxation method [27,28]. Only one relaxation peak has been observed. The activation energy of this peak increases first with W concentration and then saturates at a value of about 1.45 eV above a certain substitution range. Therefore the study of the diffusion properties in W-substituted $La_2Mo_2O_9$, which is our second goal of this work, may help us understand the mechanism for two relaxation peaks.

Pauling put forward the classic rule on ion-crystal stability in 1929 [29]. This rule can be put in a more useful form by using the extension suggested by Brown and Altermatt [30]. The valence V_i of the ith atom is given by the sum of the individual bond valences s_{ij} between it and its nearest-neighbor atoms j:

$$V_i = \sum_j s_{ij}. \tag{1}$$

The individual bond valences can be calculated from the observed bond lengths R_{ij}:

$$s_{ij} = \exp\left(\frac{R_0 - R_{ij}}{B}\right), \tag{2}$$

where R_0 is a constant dependent upon the nature of the ij pair, and $B = 0.37$. The bond valence sums (BVS) characterizes the interactions between atoms and its nearest-neighbor atoms and correlates well with the stability of the structure. Hence they are usually used to explain some perplexing problem of stability of structure. For example, Harrington et al. have used the evolution of BVS with substitution concentration to provide an explanation for the stabilization of high-temperature phase $Zn_7Sb_2O_{12}$ to lower temperature by means of cations doping [31]. In addition, Yashima et al. recently found that there is a close relationship between the site preference of doping atom and BVS values in the undoped system: the site with relatively smaller BVS values indicate the preference site for larger-sized doping atom [32]. Our third goal of this paper is to validate the correlation of the site preference of doping atom and BVS in β-$La_2Mo_2O_9$ based on first principle results.

In the present work, we use first-principles total energy calculations to study the structure properties of substituted $La_2Mo_2O_9$ and employ nudged elastic band (NEB) method and the dimer method to investigate diffusion properties of O ions in W-substituted $La_2Mo_2O_9$. The paper is organized as follows: in Section 2, we describe the method of our simulation; the results of our simulations and the corresponding discussion are reported in Section 3; a short summary is given in Section 4.

2. Computational methods

Our calculations are performed within the framework of the density-functional theory, with the PBE generalized gradient approximation to the exchange correlation energy, and the valence electron-ion interaction was modeled by the projector augmented wave potential [33,34], as implemented in the Vienna *ab initio* simulation package [35]. The atoms of system were put in a simple cubic box with periodical boundary condition. The plane wave cutoff and k-point density, obtained using the Monkhorst–Pack method [36], were both checked for convergence for each system to be within 0.001 eV per atom. Following a series of test calculations a plane wave cutoff of 700 eV was used and a k-point grid density of $2\times2\times2$ was employed. The structural optimization is truncated when the forces converge to less than 0.01 eV/Å.

In our early work, we have 12 different local or inherent structural configurations of β-$La_2Mo_2O_9$, which can be regarded as snapshots representing small regions of the disorder material and correspond to separate local minima on the potential energy hypersurface of the system [22]. We randomly selected one of these different configurations as the structure to be doped, because these different configurations are connected to each other by one of 12 point operations of $P2_13$ space group. There are eight unique cation positions (shown in Fig. 1, named a, b, c, and d for La and e, f, g, and h for Mo respectively) in β-$La_2Mo_2O_9$ due to the ordered arrangement of the oxygen-ion. So the site preference for doping atom should be firstly detected. And then, the lattice parameters of the doped β-$La_2Mo_2O_9$ are determined by performing a series of total energy calculation using different lattice parameters. Because of some dopant concentrations less than 25%, we made a 52-atom supercell β-$La_8Mo_8O_{36}$ by enlarging the 26-atom supercell with the lattice vectors $\mathbf{A} = (a\mathbf{i} + a\mathbf{j})$, $\mathbf{B} = (a\mathbf{i} - a\,\mathbf{j})$, $\mathbf{C} = a\mathbf{k}$, where a is the cell parameter. So a series of structural configurations

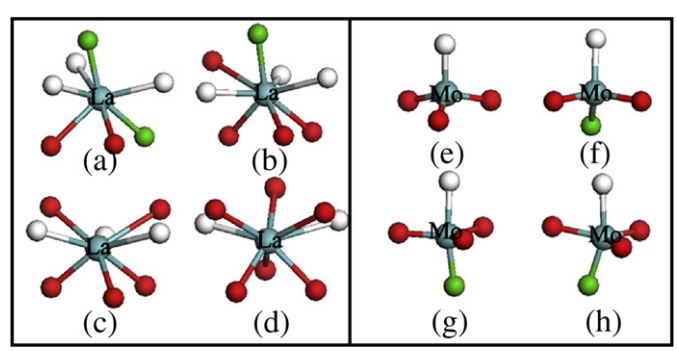

Fig. 1. Local O ion arrangements around La and Mo cations in β-$La_2Mo_2O_9$ to distinguish their differences. The O(1), O(2), and O(3) atoms are marked in white, red(dark gray), and green(gray) balls, respectively. (For interpretation of the references to color in this figure legend, the reader is referred to the web version of this article.)

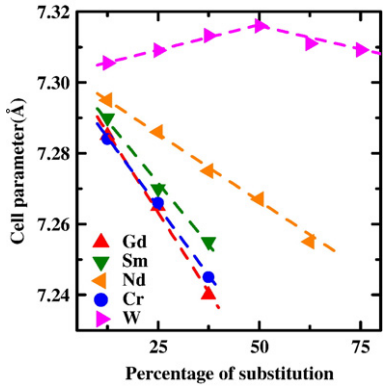

Fig. 2. Evolution upon substitution rate of the cell parameters of different doped systems. Lines are presented as guides of the eye.

of the doped β-$La_2Mo_2O_9$ were obtained for analyzing the structures evolution with substitution concentration and the β phase stability.

Based on the above calculation of structure of W-doped β-$La_2Mo_2O_9$ and our previous study of the diffusion of O ion in pure β-$La_2Mo_2O_9$, we optimized some inherent structural configurations (shown in Fig. 2 in our previous work [22]) with W-doped system, which are used as the input structures for studying the diffusion properties of O ions by the nudged elastic band (NEB) [37,38]. Here we consider those possible diffusion paths which include one O ion moving from MoO_5 hexahedra to MoO_4 tetrahedra and accompany by other O ions moving inside MoO_5 hexahedra or MoO_4 tetrahedra. The NEB method is a reliable way to find the minimum-energy paths, when the initial and final states of a process are known. An interpolated chain of configurations (images) between the initial and final positions is connected by springs and relaxed simultaneously to the minimum-energy path. With the climbing image scheme, the highest-energy image climbs uphill to the saddle point. The dimer method [39], which is designed to deal with this problem by searching for saddle points corresponding to unknown reaction mechanisms, is used to accurately converge upon a saddle point, starting from an NEB calculation. In our present work, the transition state obtained by NEB is used as the input structure of the dimer method to accurately converge upon a saddle point. In addition, we fixed the positions of all cations in all the calculations (i.e., oxygen ions are only relaxed) on the basis of the experimental results that the cation positions are located exactly and, compared to the pure system the changes in cation positions in doped systems are very small [4,15,18,20,14].

3. Results and discussions

In Tables 1 and 2 we summarize the coordination number of cations at different sites, the results of the optimized total energies and bond valence sums which are calculated by Eqs. (1) and (2) (here, $R_0 = 2.172$ Å and 1.907 Å for La^{3+} and Mo^{6+} respectively [40]). As shown in Table 1, a comparison of total energies of the doped systems among four different substitution sites indicates that, Gd, Sm and Nd atoms, whose ionic radii are smaller than that of La, prefer the crystallographic sites with largest BVS values, whereas Bi atom, whose ionic radius is slightly larger than that of La, prefers the crystallographic site with second largest BVS values. Table 2 indicates that, Cr prefers to occupy the site with a coordination number of 4, while W prefers the site with a coordination number of 5. These are rationalized in terms of the smaller-sized Cr atom and the slightly-larger-sized W atom as compared with the Mo atom. We can also see that, Cr prefers the site with the largest BVS value and W prefers the site with lower BVS value. This suggested that the BVS values in undoped system could be used as an indicator for the site preference of dopant cations: the dopant cations with relatively large ionic radius prefer to sites with smaller BVS values; while small dopant cations preferentially occupy crystallographic sites with larger BVS values. This correlation of the site preference of doping atom and BVS values is similar to that reported by Yashima and Kawaike [32]. It should be noted that the case of Bi^{3+} substitution on La^{3+} is not consistent with this regulation. We guess that it may be related to the lone-pair electrons of Bi^{3+} ion and need to be further studied in the future work.

Table 1
Coordination number (CN), bond valence sums (BVS) of cations at different sites before doping, and the total energy (E(L), in unit of eV) of the doped surpercell $La_7L_1Mo_8O_{36}$ (L = Gd, Sm, Nd and Bi).

Site	CN	BVS (La)	E (Gd)	E (Sm)	E (Nd)	E (Bi)
(a)	7(3O(1) + 2O(2) + 2O(3))	3.059	−439.43	−439.40	−439.63	−432.61
(b)	8(3O(1) + 4O(2) + 1O(3))	3.337	−439.57	−439.53	−439.74	−432.68
(c)	8(3O(1) + 5O(2))	2.992	−439.30	−439.33	−439.62	−432.70
(d)	8(2O(1) + 6O(2))	3.132	−439.35	−439.37	−439.64	−432.77

The total energy of pure $La_8Mo_8O_{36}$ is −440.06 eV.

Table 2
Coordination number (CN), bond valence sums (BVS) of cations at different sites before doping, and the total energy (E(M), in unit of eV) of the doped surpercell $La_8Mo_7M_1O_{36}$ (M = Cr, W).

Site	CN	BVS (Mo)	E (Cr)	E (W)
(e)	4(1O(1) + 3O(2))	5.707	−438.22	−442.87
(f)	4(1O(1) + 2O(2) + 1O(3))	5.731	−438.24	−442.88
(g)	5(1O(1) + 3O(2) + 1O(3))	5.645	−436.90	−443.21
(h)	5(1O(1) + 3O(2) + 1O(3))	5.571	−436.84	−443.18

Based on the above results of the site preference for different doping atoms, the cell parameters of doped systems by Gd, Sm and Nd for La and by Cr and W for Mo are calculated at their respective preference sites. The evolution of calculated cell parameters with substitution concentration is shown in Fig. 2. Trivalent Gd, Sm and Nd being smaller than trivalent La and hexavalent Cr being much smaller than hexavalent Mo, as expected the crystal cell volume is decreased upon substitution of La by Gd, Sm and Nd and substitution of Mo by Cr. The cell parameter evolution in Gd-, Sm-, Nd- and Cr-doped systems shows a linear decreasing dependence on the substitution concentration, thus following the usual Vegard's law. This is in good agreement with the experimental results [15,14,21]. In sharp contrast with the above-discussed substitution series, the cell parameter evolution upon W substitution shows a nonlinear dependence, making this series unique in the whole doped family. Since W ionic radius is slightly larger than that of Mo, it is expected that the cell parameter to slightly increase upon W substitution. It is true when the substitution content is lower than 50%. Above this value, the cell parameter surprisingly decreases. Our obtained nonlinear dependence of the cell parameter on W substitution concentration is in complete agreement with the experimental result [21]. This nonlinear dependence of cell parameter may arise from the following reasons. As have presented in Table 2, W-doping atom prefers those sites with coordination number of 5. When the substitution concentration is 50%, the sites with coordination number of 5 have all been substituted by W, any more W-doping thus makes W occupy the sites of 4 coordination. These would result in the change in the Mo/W–O bond length, so the average Mo/W–O bond length were calculated and presented as a function of the percentage of substitution in Fig. 3. From this figure, we can clearly see that Mo/W–O bond length first increases and then decrease with W content, exhibiting the similar dependence on W content as the cell parameter.

We now turn our attention to the phase stability of doped systems in terms of the cohesive energy. Fig. 4 shows the evolution upon

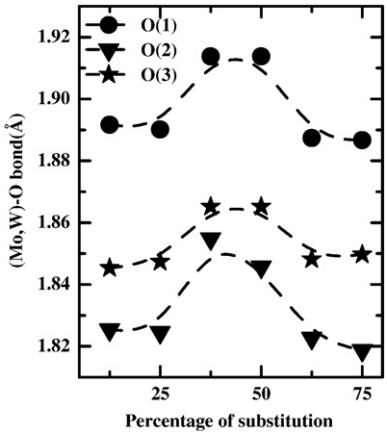

Fig. 3. Average Mo/W–O(1)/O(2)/O(3) bond length as a function of the percentage of substitution Mo by W. Lines are guide for the eye.

substitution of calculated cohesive energies in Gd-, Sm-, Nd-, Cr- and W-doped systems. From Fig. 4, we can clearly see that the cohesive energy of Gd-, Sm-, Nd- and W-doped system decreases steadily with increasing substitution concentration, indicating that the introduction of Gd, Sm, Nd and W atoms may stabilize the high-temperature phase. This is consistent with the experiment result. In contrast with the above-discussed substitution series, the cohesive energy evolution upon Cr substitution shows a linear increase with substitution concentration, which may be the reason of the experimentally observed impurity-phase $LaCrO_3$ [21].

BVS represent an extension to more complex structures of the original electrostatic valence rule of Pauling which essentially required local electroneutrality to be preserved in order for a structure to be stable, and thus correlate with the stability of the different structures. Here, in our high-temperature disorder phase of $La_2Mo_2O_9$, the expected value of BVS of La and Mo is 3 and 6, respectively. As listed in Tables 1 and 2, the BVS values of La and Mo in the high-temperature phase are 2.992–3.337 and 5.645–5.731, which are greatly larger or lower than their expected values, respectively. Note that a significant deviation of BVS values from expected values represent departure from local electroneutrality and potential instability in the structure, and this destabilization could be offset by an increase in entropy associated with structural disorder, resulting in stabilization of the structure above a certain temperature, as found here in the β phase. Hence the β phase is entropically stabilized.

We also calculated the BVS value for all cation sites in the above-discussed doped systems using Eqs. (1) and (2) (here, $R_0 = 2.172$ Å, 2.065 Å, 2.088 Å, 2.117 Å, 1.907 Å, 1.724 Å, and 1.921 Å, for La^{3+}, Gd^{3+}, Sm^{3+}, Nd^{3+}, Mo^{6+}, Cr^{6+} and W^{6+}respectively [40]). For convenient measure of the deviation of BVS values over the whole structure, we calculated the $R1$, which is the root-mean-square average of the discrepancy between expected values and calculated values of BVS [41]:

$$R1 = \langle (V_i^c - V_i)^2 \rangle^{1/2}, \tag{3}$$

where V_i^c is the expected value of cation i, V_i is the calculated values of cation i. Any decrease of the $R1$ values by means of doping would effectively reduce the extent of departure from electroneutrality and the temperature at which the entropic stabilization was required [31]. The evolution of $R1$ values with substitution concentration are shown in Fig. 5. From the figure, we can clearly see that the $R1$ values decrease with the substitution concentration in Gd-, Sm-, Nd- and W-doped system. This implies that the extent of departure from electroneutrality and the temperature required for entropic stabilization are reduced by doping with Gd, Sm, Nd and W. Hence the high-temperature β phase can be observed at lower temperature in these doped systems. For Cr-doped system, the $R1$ value increases upon substitution. This indicates that the substitution of Mo by Cr does not stabilize the high-temperature. These results are consistent with both our previous analysis based on the cohesive energy and the experimental results. It should be noted that the $R1$ values decrease rapidly in Gd- and Sm-doped system, while the $R1$ value decreases very slowly in Nd-doped system. This different behavior help us understand the experimental observation that different doped systems stabilize the β phase at different temperature as mentioned in Section 1.

To further understand the observed relaxation peaks in the mechanical and dielectric measurement, we systematically investigated the oxygen-ion diffusion property in W-doped system. The oxygen-ion transition paths can be obtained theoretically using the NEB method. The accurate energy barriers are obtained using the dimer method. Three minimum-energy transition paths are found and presented in Fig. 6. Note that two of three transition paths as shown in Fig. 6(a) and (c) are the same as Fig. 4(b) and (c) of the previous work [22], one new transition path as shown in Fig. 6(b) has been found. It should be pointed out here we do not consider the minimum path shown in Fig. 4(a) of our previous work [22], because O ions do not diffuse along the MoO-polyhedron network. As shown in Fig. 6(a), one O(2) ion moves to the unoccupied nearest-neighboring O(3) site in another MoO polyhedron [here, for convenience this motion process is simply marked with O(2)anotherO(3)] and simultaneously one O(3) ion jumps to the unoccupied nearest-neighboring O(2) site inside the same MoO polyhedron [O(3)sameO(2)]. This diffusion path is referred to as path A. Using the similar mark, we can denote the diffusion process (path B) in Fig. 6(b) by two subprocesses: O(1)sameO(2), O(2)anotherO(1). Note that here two referred O(1) sites are the same site and this site is occupied both in initial and finial states but by different O ions. The diffusion path C involves the collective

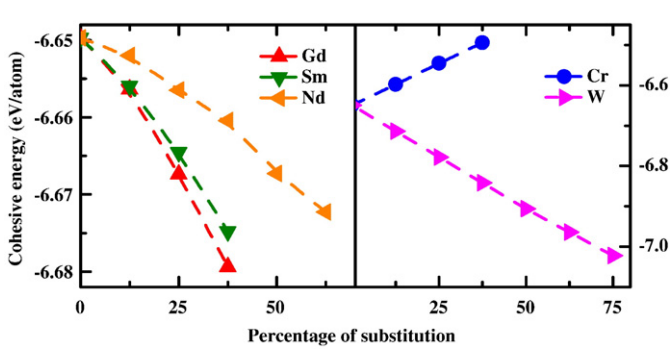

Fig. 4. Evolution upon substitution rate of the cohesive energy of different doped systems. Lines are presented as guides of the eye.

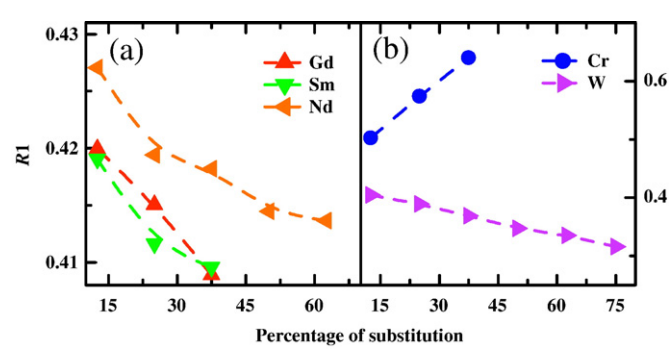

Fig. 5. Evolution upon substitution rate of $R1$ in different doped systems. Lines are presented as guides of the eye.

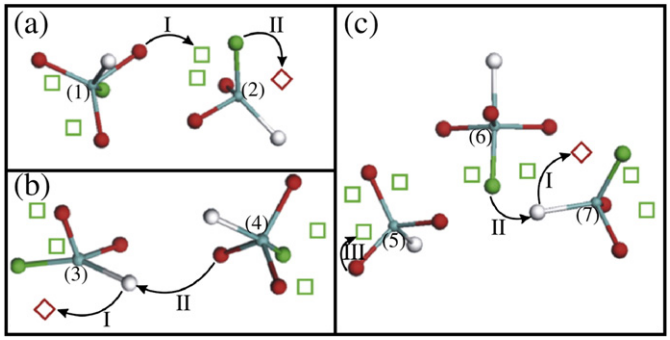

Fig. 6. Schematic diagram of typical minimum-energy transition paths connecting the local structures of W-doped systems. The O(1), O(2), O(3) and Mo/W atoms are marked in white, red (dark gray), green (gray), and small cyan (small gray) balls, respectively, and the unoccupied positions of O(2) and O(3) sites are marked in red (dark gray) and green (gray) squares, respectively. The arrows I, II, and III denote the subprocesses in the transition paths, and the start and end points of the arrow denote initial and final positions of the migration path, respectively. 25% W-doped: there exists two cases, one case is all small cyan balls are Mo atoms (O atoms move near Mo), another case is the small cyan balls denoted by (1), (4) and (6) are W atoms. 50% W-doped: the small cyan balls denoted by (1), (4) and (6) are W atoms. 75% W-doped: the small cyan balls denoted by (1)–(4), (6) and (7) are W atoms. (For interpretation of the references to color in this figure legend, the reader is referred to the web version of this article.)

motion of O(1) and O(2) and O(3) ions shown in Fig. 6(c). The path C includes three subprocesses: O(1)sameO(2), O(3)anotherO (1), O(2)sameO(3). The two referred O(1) sites here is the same with that in the path B. Only one Mo/W–O bond is broken.

The obtained migration distance of oxygen-ion and energy barrier of paths A, B and C in undoped and W-doped systems with different concentration are summarized in Table 3. The migration distance of oxygen-ion is the distance between the initial location and the final location in the subprocesses. For the pure system, we can see that, (i) the energy barrier (0.5 eV) of path A is small, suggesting the corresponding relaxation process would be activated at much lower temperature, so this case is not discussed in the following. (ii) The energy barriers of path B (1.05 eV) and C (1.24 eV) are close to the experimental results (0.9 and 1.1 eV) in the mechanical relaxation measurement, suggesting that the collective diffusion channels of B and C may be responsible for the two mechanical relaxation subpeaks P_1 and P_2, respectively. Therefore, though O(1) sites are fully occupied and O(2) and O(3) are partially occupied, O(1) ions are mobile such as O(2) and O(3) ions in both transition paths A and B. There exists a small difference in the energy barriers between these two transition paths. From Table 3, we can clear see that, W-doping leads to the obvious increase in the energy barriers for transition paths B and C, suggesting the experimentally observed relaxation peaks due to W-doping should move towards to high temperatures, which is in agreement with the experimental result [27,28]. In order to clearly display the W-content dependence of energy barrier in W-doped systems and make a comparison with the experiment, we replot in

Table 3
Migration distance D_m (Å) of oxygen ion in subprocesses and energy barriers E_b (eV) of three diffusion paths A, B and C (shown in Fig. 6) in $La_4Mo_{4-y}W_yO_{18}$ ($y = 0, 1, 2, 3$).

	Path A			Path B			Path C			
	D_m (I)	D_m (II)	E_b	D_m (I)	D_m (II)	E_b	D_m (I)	D_m (II)	D_m (III)	E_b
$La_4Mo_4O_{18}$	1.82	1.18	0.50	2.05	2.60	1.05	2.37	2.73	1.08	1.24
$La_4Mo_3W_1O_{18}$	1.90	1.11	0.81	2.07	2.68	1.22	2.41	3.16	1.02	1.36
$La_4Mo_2W_2O_{18}$	1.90	1.10	0.84	2.08	2.68	1.38	2.41	3.14	1.01	1.43
$La_4Mo_1W3O_{18}$	1.90	1.10	0.71	2.06	2.67	1.35	2.41	3.13	1.01	1.37

Note that, for the case of 25% W-doped ($La_4Mo_3W_1O_{18}$), the barrier energy is the average value of two diffusion cases (for details see the caption of Fig. 6).
I, II and III denote the subprocesses in the transition paths.

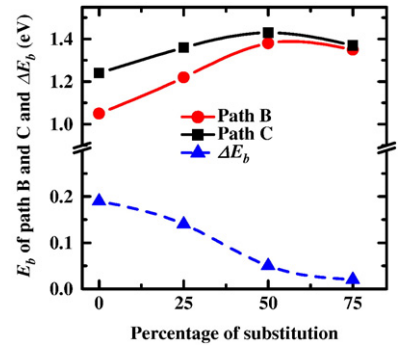

Fig. 7. The energy barrier (E_b) of transition paths B and C and their difference (ΔE_b) as a function of W content.

Fig. 7 the change tread of energy barriers in transition paths B and C in Table 3 and their difference as a function the percentage of W substitution. With increasing W content, the energy barriers of paths B and C first increase obviously then become insensitive to W content. But the difference of energy barrier between paths B and C decreases with W content, and almost disappears for the W-doped system with 75%. This evolution behavior of energy barrier with W concentration is also in accordance with the experimental result [28]. This remarkable decrease in the difference of energy barrier between B and C may be the reason that only one relaxation peak is observed in the mechanical relaxation measurement in doped system, compared to undoped system.

4. Conclusion

We have performed *ab initio* simulations to study the influences of Gd, Sm, Nd, Bi, Cr and W substitutions on the structure and phase stability of the β phase. The diffusion properties of W-doped system are also investigated using the nudged elastic band method and the dimer method. It is found that Gd, Sm and Nd atoms, whose ionic radii are smaller than that of La, prefer the crystallographic sites with largest BVS values, whereas Bi atom, whose radius is are slightly larger than that of La, prefers the crystallographic site with second largest BVS values. The results of Cr and W substitution for Mo show that Cr prefers to occupy the site with coordination number of 4, while W prefers the site with coordination number of 5. In contrast with the linear dependence in other doped systems, the cell parameter of W-doped systems shows a nonlinear dependence on W content, which results from the nonlinear change in Mo/W–O bond length with W content. The evolution of cohesive energy upon the substitution concentration indicate that the introduction of Gd, Sm, Nd and W atoms stabilize the high-temperature phase. From BVS calculations, the BVS values for all cations in the β phase are significantly deviation from the expected values, suggesting the β-$La_2Mo_2O_9$ is entropically stabilized. Substitutions of Gd, Sm, Nd and W in $La_2Mo_2O_9$ reduce the deviation of BVS values leading to stabilization of the β phase to lower temperature. Three minimum-energy transition paths in W-doped system have been studied in details. It is found: (i) W-doping leads to the obvious increase in the energy barriers for transition paths B and C, suggesting the experimentally observed relaxation peaks due to W-doping should move towards to high temperatures. (ii) There is a remarkable decrease in the difference of energy barrier between B and C, which may be the reason that only one relaxation peak is observed in the mechanical relaxation measurement in doped system, compared to undoped system.

Acknowledgments

This work was supported by the National Natural Science Foundation of China (Grant Nos. 10674135 and 50672100), and by

the Center for Computational Science, Hefei Institutes of Physical Sciences.

References

[1] K.R. Kendall, C. Navas, J.K. Thomas, H.C.Z. Loye, Solid State Ionics 82 (1995) 215.
[2] J.C. Boivin, G. Mairesse, Chem. Mater. 10 (1998) 2870.
[3] P. Lacorre, F. Goutenoire, O. Bohnke, R. Retoux, Nature (London) 404 (2000) 856.
[4] F. Goutenoire, O. Isnard, R. Retoux, P. Lacorre, Chem. Mater. 12 (2000) 2575.
[5] L. Malavasi, H.J. Kim, S.J.L. Billinge, T. Proffen, C. Tealdi, G. Flort, J. Am. Chem. Soc. 129 (2007) 6903.
[6] F. Goutenoire, R. Retoux, E. Suard, P. Lacorre, J. Solid State Chem. 142 (1999) 228.
[7] I.P. Marozau, D. Marrero-López, A.L. Shaula, V.V. Kharton, E.V. Tsipis, P. Núñez, J.R. Frade, Electrochim. Acta 49 (2004) 3517.
[8] S. Basu, P.S. Devi, H.S. Maiti, J. Electrochem. Soc. 152 A (2005) 2143.
[9] D.S. Tsai, M.J. Hsieh, J.C. Tseng, H.Y. Lee, J. Eur. Ceram. Soc. 25 (2005) 481.
[10] S. Georges, F. Goutenoire, P. Lacorre, M.C. Steil, J. Eur. Ceram. Soc. 25 (2005) 3619.
[11] C. Li, X.P. Wang, J.X. Wang, D. Li, Z. Zhuang, Q.F. Fang, Mater. Res. Bull. 42 (2007) 1077.
[12] D. Marrero-López, D. Pérez-Coll, J.C. Ruiz-Morales, J. Canales-Vázquez, M.C. Martín-Sedeno, P. Nú ñez, Electrochim. Acta 52 (2007) 5219.
[13] A. Selmi, G. Corbel, P. Lacorre, Solid State Ionics 177 (2006) 3051.
[14] S. Georges, F. Goutenoire, F. Altorfer, D. Sheptyakov, F. Fauth, E. Suard, P. Lacorre, Solid State Ionics 161 (2003) 231.
[15] D. Marrero-López, J. Canales-Vázquez, W.Z. Zhou, J.T.S. Irvine, P. Núñez, J. Solid. State Chem 179 (2006) 278.
[16] S. Georges, F. Goutenoire, Y. Laligant, P. Lacorre, J. Mater. Chem. 13 (2003) 2317.
[17] J.H. Yang, Z.H. Gu, Z.Y. Wen, D.S. Yan, Solid State Ionics 176 (2005) 523.
[18] F. Goutenoire, O. Isnard, E. Suard, O. Bohnke, Y. Laligant, R. Retoux, P. Lacorre, J. Mater. Chem. 11 (2001) 119.
[19] X.M. Gao, T.M. He, Y. Shen, J. Alloy Compd. 464 (2008) 461.
[20] J.A. Collado, M.A.G. Aranda, A. Cabeza, P. Olivera-Pastor, S. Bruque, J. Solid State Chem. 167 (2002) 80.
[21] G. Corbel, Y. Laligant, F. Goutenoire, E. Suard, P. Lacorre, Chem. Mater. 17 (2005) 4678.
[22] C.J. Hou, Y.D. Li, P.J. Wang, C.S. Liu, X.P. Wang, Q.F. Fang, D.Y. Sun, Phys. Rev. B 76 (2007) 014104.
[23] C.J. Hou, X. Zhang, C.S. Liu, X.P. Wang, Q.F. Fang, Chin. Phys. Lett. 25 (2008) 3342.
[24] X.P. Wang, Q.F. Fang, Phys. Rev. B 65 (2002) 064304.
[25] I.R. Evans, J.A.K. Howard, J.S.O. Evans, Chem. Mater. 17 (2005) 4074.
[26] S. Georges, S.J. Skinner, P. Lacorre, M.C. Steil, Dalton Trans. 19 (2004) 3101.
[27] X.P. Wang, D. Li, Q.F. Fang, Z.J. Cheng, G. Corbel, P. Lacorre, Appl. Phys. Lett. 89 (2006) 021904.
[28] D. Li, X.P. Wang, Q.F. Fang, J.X. Wang, C. Li, Z. Zhuang, Phys. stat. sol. (a) 204 (2007) 2270.
[29] L. Pauling, J. Am. Chem. Soc. 51 (1929) 1010.
[30] I.D. Brown, D. Altermatt, Acta Cryst. B 41 (1985) 244.
[31] R. Harrington, G.C. Miles, A.R. West, Mater. Res. Bull. 43 (2008) 1949.
[32] M. Yashima, Y. Kawaike, Chem. Mater. 19 (2007) 3973.
[33] J.P. Perdew, K. Burke, M. Ernzerhof, Phys. Rev. Lett. 77 (1996) 3865.
[34] P.E. Blöchl, Phys. Rev. B 50 (1994) 17953.
[35] G. Kresse, J. Furthmuller, Phys. Rev. B 54 (1996) 11169.
[36] H.J. Monkhorst, J.D. Pack, Phys. Rev. B 13 (1976) 5188.
[37] G. Henkelman, B.P. Uberuaga, H. Jónsson, J. Chem. Phys. 113 (2000) 9901.
[38] G. Henkelman, H. Jónsson, J. Chem. Phys. 113 (2000) 9978.
[39] G. Henkelman, H. Jónsson, J. Chem. Phys. 111 (1999) 7010.
[40] N.E. Brese, M. O'Keeffe, Acta Cryst. B 47 (1991) 192.
[41] I.D. Brown, Acta Cryst. B 48 (1992) 553.